AIP Advances

Role of top and bottom interfaces of a Pt/Co/AlO_x system in Dzyaloshinskii-Moriya interaction, interface perpendicular magnetic anisotropy, and magneto-optical Kerr effect

Cite as: AIP Advances **7**, 035213 (2017); https://doi.org/10.1063/1.4978867
Submitted: 08 December 2016 • Accepted: 06 March 2017 • Published Online: 15 March 2017

Nam-Hui Kim, Jaehun Cho, Jinyong Jung, et al.

AIP ADVANCES **7**, 035213 (2017)

Role of top and bottom interfaces of a Pt/Co/AlO$_x$ system in Dzyaloshinskii-Moriya interaction, interface perpendicular magnetic anisotropy, and magneto-optical Kerr effect

Nam-Hui Kim,[1] Jaehun Cho,[2] Jinyong Jung,[1] Dong-Soo Han,[3] Yuxiang Yin,[3] June-Seo Kim,[3,4,a] Henk J. M. Swagten,[3] Kyujoon Lee,[5] Myung-Hwa Jung,[6] and Chun-Yeol You[1,b]

[1]*Department of Emerging Materials Science, DGIST, Daegu 42988, South Korea*
[2]*Department of Physics, Inha University, Incheon 22212, South Korea*
[3]*Department of Applied Physics, Center for NanoMaterials, Eindhoven University of Technology, P.O. Box 513, 5600 MB Eindhoven, The Netherlands*
[4]*DGIST Research Center for Emerging Materials, DGIST, Daegu 42988, South Korea*
[5]*Institute of Physics, Johannes Gutenberg-Universität Mainz, Mainz 55099, Germany*
[6]*Department of Physics, Sogang University, Seoul 04107, South Korea*

(Received 8 December 2016; accepted 6 March 2017; published online 15 March 2017)

We investigate the role of top and bottom interfaces in inversion symmetry-breaking Pt/Co/AlO$_x$ systems by inserting ultra-thin Cu layers. Wedge-type ultrathin Cu layers (0-0.5 nm) are introduced between Pt/Co or Co/AlO$_x$ interfaces. Interface sensitive physical quantities such as the interfacial Dzyaloshinskii-Moriya interaction (iDMI) energy density, the interfacial perpendicular magnetic anisotropy (iPMA), and the magneto-optical Kerr effects (MOKE) are systematically measured as a function of Cu-insertion layer thickness. We find that the Cu-insertion layer in the bottom interface (Pt/Co) plays a more important role in iDMI, PMA, and MOKE. In contrast, the top interface (Co/AlO$_x$) noticeably contributes to only PMA, while its contributions to iDMI and MOKE enhancement are less significant. Although the PMA mainly comes from the bottom interface (Pt/Co), the Cu-insertion layers of all interfaces (Pt/Co, Co/AlO$_x$) influence PMA. For iDMI, only the Cu-insertion layer in the bottom interface exerts SOC suppression which leads iDMI energy to decrease rapidly. [http://dx.doi.org/10.1063/1.4978867]

I. INTRODUCTION

An interface is an important place in many physical phenomena, where the symmetry is broken and the boundary conditions are built in. The role of an interface in modern magnetism is crucial, and many exotic phenomena are closely related to interfaces, including giant magneto-resistance, tunneling magneto-resistance, exchange bias, spin transfer torque (STT), perpendicular magnetic anisotropy (PMA), proximity induced magnetization (PIM), and spin-orbit torque (SOT), among others. As such, interfaces are fundamental building blocks of modern spintronic devices. Recently, spin orbit coupling (SOC) between ferromagnetic (FM) and heavy metals (HM) has been re-visited due to the crucial physical origins of the spin Hall effect (SHE),[1–3] Rashba effect,[4,5] and interfacial Dzyaloshinskii-Moriya interaction (iDMI).[6–9] Since SOT requires inversion symmetry breaking, basic HM/FM/I, (I: Insulator) structures have been heavily investigated by many groups. Miron *et al.*[4] claimed the

[a]E-mail: spin2mtj@dgist.ac.kr
[b]E-mail: cyyou@dgist.ac.kr

presence of the Rashba effect in the Co/AlO_x system, which can alter the switching field, and reported that perpendicular magnetization can be switched by the Rashba effect.[5] This stimulated the study of SOT, and Liu *et al.*[10,11] found that SHE also exists in (Pt,Ta)/CoFeB/MgO systems. They measured the effective field strength of SHE using a ferromagnetic resonance (FMR) technique and found a spin Hall angle of 0.15 for beta-phase Ta. They have also reported that it is possible to switch the perpendicularly magnetized FM layer by SHE. Pioneering works paved the way to "spin-orbitronics," and they have led to many efforts to measure the effective fields by SOT.[1,12–14] More recently, Emori *et al.*[15] claimed that iDMI plays a major role in domain wall (DW) motion, and Thiaville *et al.*[16] suggested that iDMI suppresses the Walker breakdown, allowing for faster DW motion. Ryu *et al.*[17,18] also reported that DW motion is governed not only by STT, but also by SHE, iDMI and PIM. Since the proposal of topologically-protected skyrmion-based logic devices,[19] iDMI has become a central part of spin-orbitronics.[20,21] iDMI requires two conditions: the first is a strong SOC, and the second is an inversion symmetry breaking structure. In HM/FM/I systems, these two conditions are spontaneously satisfied. By non-reciprocal spin wave (SW) dispersion relations,[22] several experimental techniques have been proposed to measure iDMI. Zakeri *et al.*[23] measured iDMI energy density by employing spin-polarized electron energy loss spectroscopy (SPEELS), and Je *et al.*[24] determined the effective field due to iDMI by an asymmetric DW velocity measurement technique. Recently, Han *et al.*[25] introduced another experimental method as a magneto static measurement for probing exist of iDMI from asymmetric hysteresis loop shift, and several groups reported iDMI of HM/FM/I systems using Brillouin light scattering (BLS).[26–30] Most studies have been focused on the determination of the iDMI energy density of the whole inversion symmetry breaking system. Despite all of the above efforts, the role of top (FM/I) and bottom (HM/FM) interfaces of HM/FM/I system have not yet clearly been studied.

In this report, we investigate the contribution of each top and bottom interface to the iDMI, PMA, and MOKE amplitude modulations as an inserted ultra-thin Cu layer (0-0.5 nm) in the HM/FM or FM/I interface. We find that iDMI and PMA rapidly disappear with increasing Cu-insertion layer thickness in the bottom (HM/FM) interface, whereas iDMI and PMA maintain their values regardless of the Cu-thickness in the top (FM/I) interface. The MOKE amplitude requires more complicated multiple reflections analysis with correct optical and magneto-optical properties to make clear conclusions,[31,32] however, it is clear that the Cu-insertion layers in the top and bottom interfaces change MOKE amplitude more drastically than simple magneto-optical analysis, indicating that the optical and/or magneto-optical properties are significantly altered.

II. SAMPLE PREPARATION

In order to observe the role of the inserted Cu layer, we prepare two wedge-shaped samples on the top of a thermally-oxidized Si/SiO_2 wafer. The wedge sample structures were Si/SiO_2/Pt (4 nm)/Cu (0.0-0.5 nm)/Co (1.1 nm)/AlO_x (2 nm) and Si/SiO_2/Pt (4 nm)/Co (1.1 nm)/Cu (0.0-0.5 nm)/AlO_x (2 nm) as shown in Fig. 1 (a) and (b) (inset). Hereafter, we refer to the samples, where a Cu layer with a thickness variation of 0.0-0.5-nm was inserted between Pt/Co and Co/AlO_x, as "BOTTOM" and "TOP," respectively. All samples were prepared by DC magnetron sputter at a base pressure of $\sim 7\times10^{-8}$ mbar. The wedge-shaped Cu layers were grown using a moving *in-situ* linear shadow mask. Here, we would like note that although the thickness of the Cu layers in the two samples were prepared to be nominally the same, the unintended offset in their thickness could also have arisen due to the shadow effect and/or the difficulty in precisely adjusting the mask to a certain position. The AlO_x layer was prepared by plasma oxidation of the 2-nm thick Al layer (see our previous works[26,33] for precise details).

We chose Cu as an insertion layer for several physical reasons. One, it is well known that Cu is immiscible with Co,[34] while Pt is highly miscible with Co.[35] Recently, it has been reported experimental and theoretical study for Co diffusion in the few atomic layer of Cu only at the high temperature,[36] and Bandiera *et al.* also systematically studied for PMA and reducing inter-diffusion at Co/Pt multilayer structures by inserting an ultra-thin Cu layer which leads to a well-defined layered stack with enhanced anisotropy.[37–39] Furthermore, it has greatly discussed and clarified long times ago by B. Hillebrands for many anisotropic systems such as the stabilization of ferromagnetic order

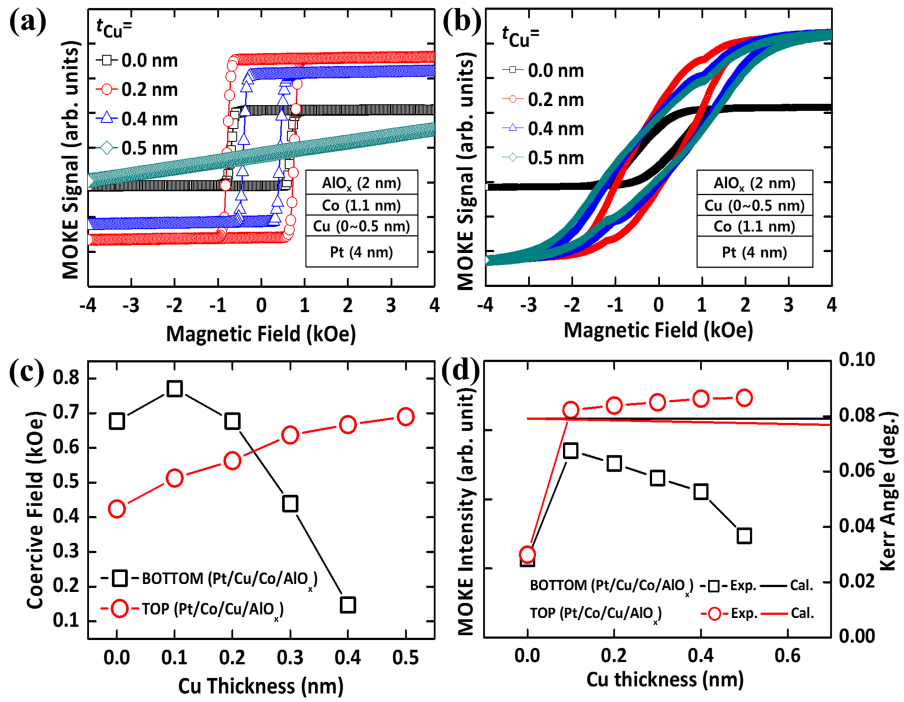

FIG. 1. Structures of wedge Cu-insertion layer samples (inset) and MOKE hysteresis loops (a) BOTTOM: Si/SiO_2/Pt (4 nm)/Cu (0.0-0.5 nm)/Co (1.1 nm)/AlO_x (2 nm); (b) TOP: Si/SiO_2/Pt (4 nm)/Co (1.1 nm) /Cu (0.0-0.5 nm)/AlO_x (2 nm); (c) coercivity; and (d) saturation MOKE signal with calculated MOKE angles (solid lines) with medium boundary/propagation matrix method for BOTTOM and TOP samples as a function of t_{Cu}.

by in-plane anisotropy, induced uniaxial anisotropy and strain-induced suppression of the magneto-crystalline anisotropy in Co/Cu structure.[40,41] Therefore, we can minimize structural disorder and the possibility of alloying by Cu-insertion layer. Moreover, the SOC of Cu is negligible, so the Cu-layer acts as an effective SOC breaker. However, due to the long spin diffusion length of Cu (> 500 nm), a thin Cu layer is seen as transparent for the spin current. And spin memory loss (SML δ) also has been reported at various interfaces between non-magnetic metal and ferromagnetic layers such as Pd/Co(δ= 0.24), Pt/Cu(δ= 0.9),[42] Co/Pt(δ= 0.25),[43] and Co/Pt(δ= 0.9)[44] structures. The SML parameter is determined by space layer thickness (t_I) and the spin diffusion length (ℓ^I_{sf}), however, the thickness range of Cu layer in our sample structure is only from 0 to 0.5 nm, so the SML parameter is very small (δ= ~10^{-3}). Consequently, the interfacial SML effect does not crucial point in our experiment, and we can claim that the Cu insertion layer is transparent for the spin current. Recently, Fan *et al.*[45] studied a Ti/CoFeB/Cu/Pt system as a function of Cu-insertion layer thickness (0-3 nm). They found that the spin Hall effect generated field like SOT, decreased slowly, while damping like SOT rapidly dropped with the Cu-insertion layer.

III. MAGNETO OPTICAL KERR EFFECT (MOKE) MEASUREMENT

We measure the magneto-optical Kerr effect (MOKE) hysteresis loops for the BOTTOM and TOP samples as a function of Cu-insertion thickness (t_{Cu}), as shown in Fig. 1 (a) and (b). For the case of the BOTTOM samples, the hysteresis loops for t_{Cu} = 0-0.4 nm showed perfect square shapes, indicating a perpendicularly magnetized structure, but, at t_{Cu} = 0.5 nm, an in-plane magnetization at its remanence state abruptly appeared. For the case of the TOP samples, the slanted hysteresis loops, of which the squareness was less than 1, were found for all Cu thicknesses. Here, we note that hysteresis loops in the BOTTOM and TOP samples of t_{Cu} = 0 nm, which are nominally the same, showed different behaviors. This might be due to the difference in the thickness offset of the Cu-inserting layer between the two sample structures as aforementioned. Although the difference in

the thickness offset may have slightly affected the quantitative analysis in the results, we expect that it did not make a significant difference in our qualitative analysis and main claims, which will be discussed later.

In Figures 1 (c) and (d), coercivities and the intensities of the MOKE signals at the saturation state of the two sample structures are plotted as a function of t_{Cu}, respectively. It is found that the coercivity of the BOTTOM sample increased when a Cu layer of $t_{Cu} = 0.1$ nm was introduced, and it decreased as t_{Cu} increased for $t_{Cu} > 0.1$ nm. The decrease of the coercive field with increasing t_{Cu} in the BOTTOM sample can be understood simply by the fact that the inserted Cu layer between Pt and Co reduced SOC at the interface, which is an essential ingredient for PMA, as further confirmed by the effective anisotropy energies (K_{eff}) vs. t_{Cu} in Fig. 2. For the TOP samples, the gradual increments of the coercivities with increasing t_{Cu} was found for all thickness ranges. In both sample structures, it is found that the intensity of the MOKE signal abruptly increased as the 0.1 nm-thick Cu layer was introduced, as shown in Fig. 1(d). But, for $t_{Cu} > 0.1$ nm, contrasting behaviors between the TOP and BOTTOM sample were found; for the case of the TOP samples, the intensity of the MOKE slowly increased with increasing t_{Cu}, but it rapidly decreased for the BOTTOM samples. In order to understand the behavior as observed in the intensity of MOKE vs. t_{Cu}, we numerically calculated the Kerr rotation angle for the incident beam injected normally into the BOTTOM and TOP interfaces, employing a medium boundary/propagation matrix method.[31,32] In the calculation, we used the optical and magneto-optical constants for the bulk values of the given materials,[31,32] $Q = 0.0376 + 0.0066i$, and complex refractive indices of AlO_x, Co, Cu, Pt, SiO_2, and Si at 633 nm which correspond to 1.717, 0.272 + 3.24i, 2.19 + 4.11i, 2.30 + 4.07i, 1.4567, and 3.882 + 0.019i, respectively,[46] and we assumed a perfect interface state. The calculated results are depicted in Fig. 1(d) with black (BOTTOM) and red (TOP)

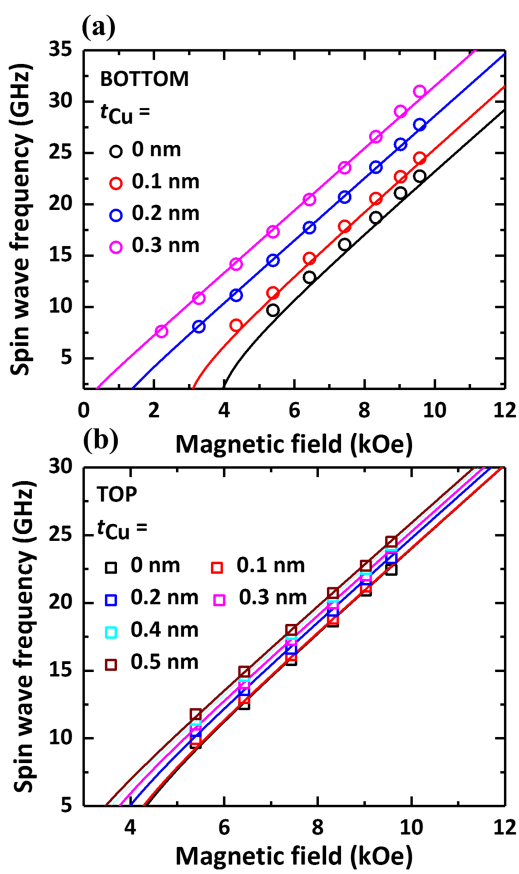

FIG. 2. SW frequencies with fitted curve (solid lines) as a function of external magnetic field (H_{ext}) for (a) BOTTOM (Pt/Cu/Co/AlO_x and open dots) and (b) TOP (Pt/Co/Cu/AlO_x and open squares) samples.

solid lines with experimental results. The numerically calculated Kerr angle based on the magneto-optical Fresnel coefficients shows quantitative deviation from the experimental measurement results, implying that the optical and magneto-optical constants significantly deviated from the bulk values as the Cu layer was introduced.

Explanation for the rapid decrease of the intensity of the MOKE signal as measured in the BOTTOM sample can be given by the suppression of the hybridization between Pt 5*d* band and Co by the ultra-thin Cu-insertion layer in the BOTTOM sample. The band hybridization contribution, which plays an important role in the MOKE spectra for Co/Pt layer, is effectively blocked by the Cu-insertion layer; thereby, the intensity of the MOKE signal drastically decreases with increasing Cu-insertion layer thickness. The increment of the MOKE intensity as found in the TOP sample can be explained by multiple reflection effects in the multilayer. For the case of the intensity of the MOKE signal, the amplitudes of the numerically calculated data are generally comparable to that of the experimental data. However, we found that the numerical calculation data shows significantly different intensity, again, probably due to the refractive indices which can be significantly differed by the formation of the films. Furthermore, we would like to note that the Cu-insertion layer could help prevent oxidation of Co from the plasma oxidation process. Even if the oxidation process is carefully performed at optimal conditions, the Co can be oxidized slightly at the interface between the Co and AlO_x layer. When the Cu layer is introduced between the Co and AlO_x layers, the formation of the CoO layer could be further prevented and may contribute to the change of the reflection in the multilayers. Although the different behaviors in the hysteresis loops between the BOTTOM and TOP samples are not fully understood in the current analysis because of the technical difficulty in investigating further, we would like to note that it is clear that the SOC between Co and Pt (BOTTOM) is more markedly influenced by the Cu-insertion layer than that between Co and AlO_x (TOP).

IV. BRILLOUIN LIGHT SCATTERING (BLS) MEASUREMENT

In order to obtain spin dynamic properties such as effective magnetic anisotropy (K_{eff}) and iDMI energy density (D), we performed BLS measurements. From the systematic BLS measurements, we obtain SWs resonance spectra (not shown here), and then we depict SWs frequencies (dots and squares) with fitted curve (solid lines) as a function of external in-plane magnetic field (f_{SW} vs. H_{ext}) in Figure 2 (a) and (b). Here, the SW frequencies without contribution of iDMI are average values between Stokes and anti-Stokes region. From the SWs frequencies results, we deduce effective saturation magnetization $\left(M_{\mathrm{eff}} = M_{\mathrm{S}} - \frac{4K_{\mathrm{S}}}{\mu_0 M_{\mathrm{S}} t_{\mathrm{FM}}}\right)$ from the following equation, $f_{\mathrm{SW}} = \frac{\gamma}{2\pi}\sqrt{H_{\mathrm{ex}}\left(H_{\mathrm{ex}} - M_{\mathrm{S}} + \frac{4K_{\mathrm{S}}}{\mu_0 M_{\mathrm{S}} t_{\mathrm{FM}}}\right)}$.[47]

Based on experimental result of SWs frequencies, we depicted the K_{eff} of BOTTOM and TOP samples as functions of the Cu-insertion layer in Fig. 3. The K_{eff} of TOP sample is slowly decaying with t_{Cu}, from 2×10^5 (t_{Cu} = 0 nm) to 1.5×10^5 J/m^3 (t_{Cu} = 0.5 nm), while K_{eff} of BOTTOM sample

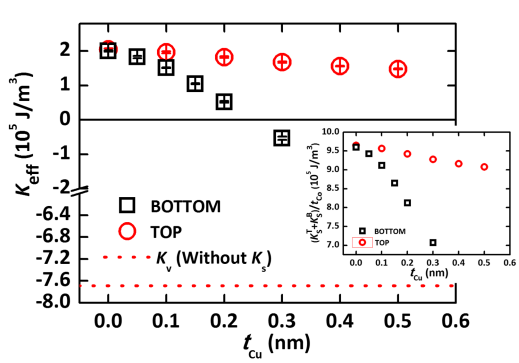

FIG. 3. Effective uniaxial anisotropy (K_{eff}) as a function of t_{Cu} for BOTTOM and TOP samples with error bars. The positive K_{eff} implies perpendicular easy axis, and K_{v} is volume anisotropy. Effective uniaxial anisotropy contributed volume anisotropy energy (inset).

rapid decays from 2×10^5 (t_{Cu} = 0 nm) to -0.5×10^5 J/m^3 (t_{Cu} = 0.3 nm). At a glance, the contribution to the PMA from top interface is not negligible, however not significant, and the PMA of the system mainly came from the bottom Pt/Co interface. In order to get more deep physical insight, we can start from the well-known relation of

$$K_{\text{eff}} = \frac{K_S^T + K_S^B}{t_{Co}} - \frac{1}{2}\mu_0 M_S^2, \tag{1}$$

where K_S^T and K_S^B are the surface anisotropy energies of TOP and BOTTOM interfaces, and μ_0 and M_S are vacuum permeability and the saturation magnetization. In order to define the effective anisotropy energy values, the saturation magnetization value is required. In the BLS measurement, the ferromagnetic layer thickness dependent measurements are required in order to determine the saturation magnetization precisely.[26,27] However, in our sample structure (Pt/Cu/Co/AlO_x and Pt/Co/Cu/AlO_x), since Co thickness is fixed, so we have to use the saturation magnetization (1.1±0.1×10^6 A/m) from our previous published report for the nominally the same sample structure.[26] From Fig. 3, we obtained $\Delta K_{\text{eff}}^T = K_{\text{eff}}^T(t_{Cu} = 0) - K_{\text{eff}}^T(t_{Cu} = 0.5) = 0.5 \times 10^5$ J/m^3 for the TOP interface, and $\Delta K_{\text{eff}}^B = K_{\text{eff}}^B(t_{Cu} = 0) - K_{\text{eff}}^B(t_{Cu} = 0.3) = 2.5\times10^5$ J/m^3 for the BOTTOM interface, respectively. If we assume that K_{eff} only varied by the corresponding surface term when we add Cu-insertion layer, we can obtain

$$\Delta K_{\text{eff}}^{B,T} = \frac{\Delta K_S^{B,T}}{t_{Co}}. \tag{2}$$

With Eq. (2), we can extract $\Delta K_S^T = 0.063$ mJ/m^2 and $\Delta K_S^B = 0.279$ mJ/m^2 for t_{Co}= 1.1 nm. It must be noted that if there is no surface anisotropy, then $K_{\text{eff}} = -\frac{1}{2}\mu_0 M_S^2$ = -7.6×10^5 J/m^3 for M_S = 1.1×10^6 A/m, it is shown in Fig. 3 as red horizontal dotted line.[26] Therefore, if 1∼2 ML Cu-insertion layer completely suppressed corresponding PMA, we can obtain $K_{\text{eff}}^T(t_{Cu} = 0.5\text{ nm})\Big|_{\text{Exp.}} = \frac{K_S^B + (K_S^T = 0)}{t_{Co}} - \frac{1}{2}\mu_0 M_S^2$ = 1.5×10^5 J/m^3, and it leads K_S^B = 1.0 mJ/m^2, and $K_{\text{eff}}^B(t_{Cu} = 0.3\text{ nm})\Big|_{\text{Exp.}} = \frac{(K_S^B = 0) + K_S^T}{t_{Co}} - \frac{1}{2}\mu_0 M_S^2$ = −0.5×10^5 J/m^3, and it leads K_S^T=0.78 mJ/m^2, respectively. However, if we substituted the K_S^B and K_S^T values to Eq. (1), we got K_{eff} = 9.3×10^5 J/m^3, and it is far from the experimentally observed values of 2.0×10^5 J/m^3. Even though if we adjust the M_S within the reasonable ranges, the discrepancy will be not disappeared. Therefore, only possible conclusion is that the 1∼2 ML Cu-insertion layer is not thick enough to effectively block the PMA between Pt/Co and Co/AlO_x. Based on above analysis, we can conclude that the contribution to the PMA from both interfaces are still significant with 1∼2 ML Cu-insertion layer, however, Cu-insertion layer blocked the PMA more effectively for the bottom Pt/Co interface, but not perfectly. For more clear understanding, we depict interface anisotropy term only, $K_{\text{eff}} + \frac{1}{2}\mu_0 M_S^2 = \frac{K_S^T + K_S^B}{t_{Co}}$, as a inset of Fig. 3. If the TOP/BOTTOM interface anisotropies disappeared, it must approach to zero values.

Another possible explanation is forming Cu clusters at the interface rather than atomically flat Cu layer for the experimental observation in Fig. 3. However, we rule out the forming Cu clusters scenario by following reason. In order to form the clusters with nominally 0.2∼0.3 nm thick Cu layer, more than 50 % of interface must be Pt/Co without Cu-insertion layer, because the clusters must be thicker than monolayer. In this case, if we assume simple area weighted average model, $K_{\text{eff}} = \eta\, K_{\text{eff, Pt/Co}} + (1 - \eta)\, K_{\text{eff, Cluster}}$, where η is fraction of Pt/Co interface, and $K_{\text{eff, Pt/Co}}$ and $K_{\text{eff, Cluster}}$ are K_{eff} value of Pt/Co and Cu cluster interface. If the half interfaces are Pt/Co and Pt/Cu(2 ML)/Co, respectively, we can assume η= 0.5, then $K_{\text{eff, Cluster}} = -\frac{\mu_0}{2}M_S^2$, and $K_{\text{eff, Pt/Co}} = \frac{K_S}{t_{Co}} - \frac{\mu_0}{2}M_S^2$, we obtained

$$K_{\text{eff}}(t_{Cu} = 1\text{ ML}) = \frac{1}{2}\left(\frac{K_S}{t_{Co}} - \frac{\mu_0 M_S^2}{2} - \frac{\mu_0 M_S^2}{2}\right) = \frac{1}{2}\left(K_{\text{eff}}(t_{Cu} = 0\text{ nm}) - \frac{\mu_0 M_S^2}{2}\right). \tag{3}$$

It gives K_{eff} = −2.7×10^5 J/m^3, which is much smaller than experimentally observed $K_{\text{eff}} \sim 0$. Therefore, we can conclude that the BOTTOM Cu-insertion layer forms atomically flat layer. Furthermore, the analysis of iDMI in next paragraph is another supporting evidence of our above explanation.

Let us discuss about the iDMI. It is well known that there are non-reciprocal SWs dispersion relations due to the finite iDMI.[22] Let f_0 is the SW frequency without iDMI, and the SW frequency with iDMI is given by:

$$f_{\mathrm{DMI}} = f_0 \pm \frac{\gamma D}{\pi M_{\mathrm{S}}} k_{\mathrm{x}}. \tag{4}$$

Here, γ is the gyromagnetic ratio, D is the iDMI energy density, and k_{x} is the SW wave vector. Without iDMI, f_0 is an even function of k_{x}; however, iDMI adds a linear term of k_{x} in the SW frequencies. We performed SW dispersion relation measurements with BLS. From systematic BLS measurements, we obtained D_{k} from the slope of the SW dispersion relations as a function of k_{x} for each Cu-insertion layer thickness as shown in Fig. 4 (a) and (b). When the Cu insertion layer located at the both BOTTOM and TOP, all dispersion relations have asymmetric properties, which clearly indicate that all samples have finite iDMI. However, variations of SW frequencies at the BOTTOM sample are large than those of them at the TOP one. These facts clearly show that the Cu insertion layer affect to interface at the Pt/Co more seriously. As a result, it implies that the Cu layer is play the role of effective SOC breaker. We also measured the external magnetic field dependence of $\Delta f = f_{\mathrm{S}} - f_{\mathrm{AS}} = \frac{2\gamma D}{\pi M_{\mathrm{S}}} k_{\mathrm{x}}$, where Δf is the frequency difference between f_{S} and f_{AS}, which correspond to the SW creation (Stokes) and annihilation (anti-Stokes) processes (not shown), respectively. From both the SW wave vector and external magnetic field dependence measurements, we obtained the iDMI energy densities corresponding to spin wave vector (D_{k}) and external magnetic field (D_{H}) variations at the BOTTOM and TOP samples as a function of t_{Cu} as shown in Fig. 5 with error bars. The agreement between D_{k} and D_{H} are excellent, and this indicates the reliability of our BLS measurements. More details of BLS measurements have been described in our previous reports.[26,27,33]

From Fig. 5, we found that the iDMI energy density of the TOP sample did not change with the thickness variation of the Cu-insertion layer. This is a clear indication that the source of iDMI comes from the Pt/Co (BOTTOM) interface, which also shows a rapid decay of iDMI energy densities for

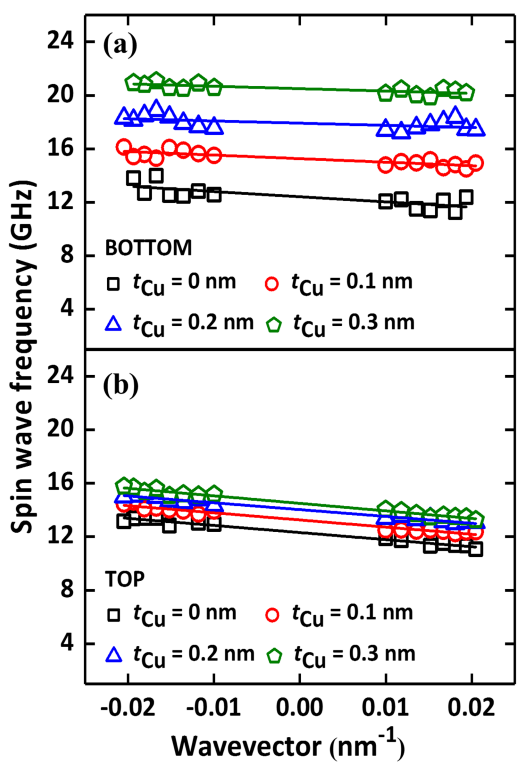

FIG. 4. Asymmetrical SWs dispersion relations as a function of wave vector (k_{x}) for (a) BOTTOM (Pt/Cu/Co/AlO$_{\mathrm{x}}$) and (b) TOP (Pt/Co/Cu/AlO$_{\mathrm{x}}$) samples in same scale.

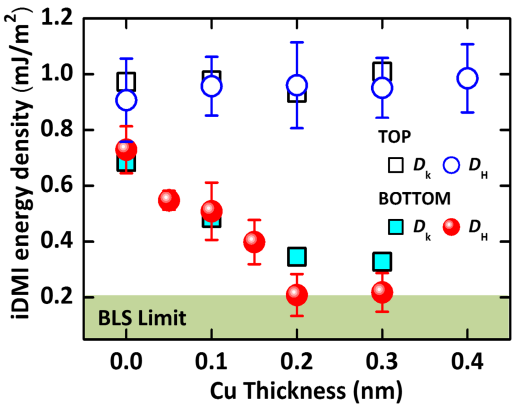

FIG. 5. iDMI energy density from SW dispersion relations (D_k) and external magnetic field dependence measurements (D_H) for BOTTOM and TOP samples as a function of t_{Cu}. The shaded area indicates BLS measurement limit (< 0.2 mJ/m^2).

the BOTTOM samples with increasing t_{Cu}. With 0.2-0.3 nm thick t_{Cu}, the iDMI is almost suppressed. Since the BLS detection limit is around 0.2 mJ/m^2, the iDMI energy densities have no meaning at the t_{Cu} = 0.2 and 0.3 nm thickness. This implies the 0.2 and 0.3 nm thick Cu-insertion layers effectively blocked SOC between the Pt and Co layers and suppressed the iDMI. When we discussed K_{eff} in Fig. 3, we ruled out the possibility of Cu cluster forming. The iDMI results support our previous conclusion. If Cu clusters are formed at the interface, then certain parts of the interface must be Pt/Co without a Cu layer, and it must have a finite iDMI. However, iDMI is negligible with a 0.2-0.3 nm Cu-insertion layer, implying that the Cu-insertion layer effectively covered the interface and it is atomically flat. Since iDMI and PMA are closely related to SOC from Pt and Cu-insertion layers terminate SOC between Pt and Co layers, it is expected that iDMI and PMA have the same variation with the Cu-insertion layer. However, the Cu-insertion layer effectively blocked iDMI with one monolayer Cu, while PMA was not fully suppressed. More detailed first principle-based theoretical work must be addressed in order to reveal the role of the Cu-insertion layer in iDMI and PMA.

V. CONCLUSIONS

We investigate the role of the interfaces between Co and Pt (BOTTOM) or Co and AlO_x (TOP) in an inversion symmetric breaking Pt/Co/AlO_x system. Various SOC coupling related phenomena such as the interfacial Dzyaloshinskii-Moriya interaction, perpendicular magnetic anisotropy, and magneto-optical Kerr effect are studied as a function of the 0-0.5 nm thick Cu insertion layers for BOTTOM and TOP interfaces, respectively. Based on our experimental data, we conclude that the PMA from the bottom interface (Pt/Co) is not totally blocked by a 1-2 ML thick Cu-insertion layer, while iDMI energy from (Pt/Co) is clearly suppressed with a 1-2 ML thick Cu-insertion layer. These facts clearly indicate that iDMI and PMA mainly came from the BOTTOM interface (Pt/Co); however, PMA and iDMI go different ways despite the same physical origin, SOC.

ACKNOWLEDGMENTS

This work is supported by the National Research Foundation of Korea (NRF) (Grant Nos. 2015M3D1A1070465, and 2014K2A5A6064900), DGIST R&D Program of the Ministry of Science, ICT and Future Planning (17-BT-02), the Leading Foreign Research Institute Recruitment Program (Grant No. 2012K1A4A3053565) through the NRF funded by the Ministry of Education, Science and Technology (MEST), and the research program of the Foundation for Fundamental Research on Matter, which is part of the Netherlands Organisation for Scientific Research.

[1] J. Kim, J. Sinha, M. Hayashi, M. Yamanouchi, S. Fukami, T. Suzuki, S. Mitani, and H. Ohno, Nat. Mater. **12**, 240 (2013).
[2] K.-W. Kim and H.-W. Lee, Nat. Phys. **10**, 549 (2014).
[3] L. Liu, C.-F. Pai, Y. Li, H. W. Tseng, D. C. Ralph, and R. A. Buhrman, Science **336**, 555 (2012).

[4] I. M. Miron, T. Moore, H. Szambolics, L. D. Buda-Prejbeanu, S. Auffret, B. Rodmacq, S. Pizzini, J. Vogel, M. Bonfim, A. Schuhl, and G. Gaudin, Nat. Mater. **10**, 419 (2011).
[5] I. M. Miron, K. Garello, G. Gaudin, P.-J. Zermatten, M. V. Costache, S. Auffret, S. Bandiera, B. Rodmacq, A. Schuhl, and P. Gambardella, Nature **476**, 189 (2011).
[6] T. Moriya, Phys. Rev. **120**, 91 (1960).
[7] I. E. Dzyaloshinshii, Sov. Phys. JETP **5**, 1259 (1957).
[8] I. E. Dzyaloshinshii, Sov. Phys. JETP **20**, 665 (1965).
[9] A. Fert and P. M. Levy, Phys. Rev. Lett. **44**, 1538 (1980).
[10] L. Liu, C.-F. Pai, Y. Li, H. W. Tseng, D. C. Ralph, and R. A. Buhrman, Science **336**, 555 (2012).
[11] L. Liu, O. J. Lee, T. J. Gudmundsen, D. C. Ralph, and R. A. Buhrman, Phys. Rev. Lett. **109**, 096602 (2012).
[12] X. Fan, H. Celik, J. Wu, C. Ni, K.-J. Lee, V. O. Lorenz, and J. Q. Xiao, Nat. Comm. **5**, 3042 (2013).
[13] H.-R. Lee, K. Lee, J. Cho, Y.-H. Choi, C.-Y. You, M.-H. Jung, F. Bonell, Y. Shiota, S. Miwa, and Y. Suzuki, Sci. Rep. **4**, 6548 (2014).
[14] M. Jamali, K. Narayanapillai, X. Qiu, L. M. Loong, A. Manchon, and H. Yang, Phys. Rev. Lett. **111**, 246602 (2013).
[15] S. Emori, U. Bauer, S.-M. Ahn, E. Martinez, and G. S. D. Beach, Nat. Mater. **12**, 611 (2013).
[16] A. Thiaville, S. Rohart, É. Jué, V. Cros, and A. Fert, Europhy. Lett. **100**, 57002 (2012).
[17] K.-S. Ryu, L. Thomas, S.-H. Yang, and S. Parkin, Nat. Nanotechnol. **8**, 527 (2013).
[18] K.-S. Ryu, S.-H. Yang, L. Thomas, and S. S. P. Parkin, Nat. Commun. **5**, 3910 (2014).
[19] A. Fert, V. Cros, and J. Sampaio, Nat. Nanotechnol. **8**, 152 (2013).
[20] X. Zhang, M. Ezawa, and Y. Zhou, Sci. Rep. **5**, 9400 (2015).
[21] J. Sampaio, V. Cros, S. Rohart, A. Thiaville, and A. Fert, Nat. Nanotechnol. **8**, 839 (2013).
[22] J. H. Moon, S. M. Seo, K. J. Lee, K. W. Kim, J. Ryu, H. W. Lee, R. D. McMichael, and M. D. Stiles, Phys. Rev. B **88**, 184404 (2013).
[23] K. Zakeri, Y. Zhang, T. H. Chuang, and J. Kirschner, Phys. Rev. Lett. **108**, 197205 (2012).
[24] S.-G. Je, D.-H. Kim, S.-C. Yoo, B.-C. Min, K.-J. Lee, and S.-B. Choe, Phys. Rev. B **88**, 214401 (2013).
[25] D.-S. Han, N.-H. Kim, J.-S. Kim, Y. Yin, J.-W. Koo, J. Cho, S. Lee, M. Kläui, H. J. M. Swagten, B. Koopmans, and C.-Y. You, Nano Lett. Accepted (2016).
[26] J. Cho, N.-H. Kim, S. Lee, J.-S. Kim, R. Lavrijsen, A. Solignac, Y. Yin, D.-S. Han, N. J. J. van Hoof, H. J. M. Swagten, B. Koopmans, and C.-Y. You, Nat. Comm. **6**, 7635 (2015).
[27] N.-H. Kim, D.-S. Han, J. Jung, J. Cho, J.-S. Kim, H. J. M. Swagten, and C.-Y. You, Appl. Phys. Lett. **107**, 142408 (2015).
[28] H. T. Nembach, J. M. Shaw, M. Weiler, E. Jué, and T. J. Silva, Nat. Phys. **11**, 825 (2015).
[29] K. Di, V. L. Zhang, H. S. Lim, S. C. Ng, M. H. Kuok, J. Yu, J. Yoon, X. Qiu, and H. Yang, Phys. Rev. Lett. **114**, 047201 (2015).
[30] N.-H. Kim, J. Jung, J. Cho, D.-S. Han, Y. Yin, J.-S. Kim, H. J. M. Swagten, and C.-Y. You, Appl. Phys. Lett. **108**, 142406 (2016).
[31] J. Zak, E. R. Moog, C. Liu, and S. D. Bader, Phys. Rev. B **43**, 6423 (1991).
[32] C.-Y. You and S. Shin, J. Magn. Magn. Mater. **198-199**, 573 (1999).
[33] N.-H. Kim, J. Jung, J. Cho, D.-S. Han, Y. Yin, J.-S. Kim, H. J. M. Swagten, and C.-Y. You, Appl. Phys. Lett. **108**, 142406 (2016).
[34] B. T. Nishizawa and K. Ishida, Bull. Alloy Phase Diag. **5**, 161 (1984).
[35] R. M. Bozorth, *Ferromagnetism*, New York, Van Nostrand (1951).
[36] T. Siahaan, O. Kurnosikov, H. J. M. Swagten, B. Koopmans, S. V. Kolesnikov, A. M. Saletsky, and A. L. Klavsyuk, Phys. Rev. B **94**, 195435 (2016).
[37] S. Bandiera, R. C. Sousa, B. Rodmacq, L. Lechevallier, and B. Dieny, J. Phys. D. Appl. Phys. **46**, 485003 (2013).
[38] S. Bandiera, R. C. Sousa, B. Rodmacq, and B. Dieny, Appl. Phys. Lett. **100**, 142410 (2012).
[39] S. Bandiera, R. R. Sousa, B. Rodmacq, and B. Dieny, IEEE Magn. Lett. **2**, 3000504 (2011).
[40] B. Hillebrands *et al.*, Acta Physica Polonica A **85**, 179 (1994).
[41] B. Hillebrands, *Brillouin Light Scattering from Layered Magnetic Structures*, Light Scattering in Solids VII, p.174 (2000).
[42] H. Kurt, R. Loloee, K. Eid, W. P. Pratt, and J. Bass, Appl. Phys. Lett. **81**, 4787 (2002).
[43] K. Eid, D. Portner, J. A. Borchers, R. Loloee, M. A. Darwish, M. Tsoi, R. D. Slater, K. V. O'Donovan, H. Kurt, W. P. Pratt, and J. Bass, Phys. Rev. B **65**, 054424 (2002).
[44] H. Y. T. Nguyen, W. P. Pratt, Jr., and J. Bass, Jour. Mag. Mag. Mater. **361**, 30–33 (2014).
[45] X. Fan, H. Celik, J. Wu, C. Ni, K.-J. Lee, V. O. Lorenz, and J. Q. Xiao, Nat. Commun. **5**, 3042 (2014).
[46] *Handbook of Optical Constants of Solids* edited by D. Palik, Academic Press, Inc. (1995).
[47] J. R. Dutcher, B. Heinrich, J. F. Cochran, D. A. Steigerwald, and W. F. J. Egelhoff, Jr., Appl. Phys. **63**, 3464–3466 (1988).